



# Laboratory and Field Evaluations of Geocell Reinforced Bases for Locally Available Material in the Himalayan Region

Bharath Gottumukkala<sup>1</sup> · Bharatram Mehar<sup>2</sup> · Divakar Minchala<sup>2</sup> · Subramanya Prasad Pulikanti<sup>3</sup> · Kranthi Kumar Kuna<sup>2</sup>

Received: 20 February 2023 / Accepted: 13 October 2023 / Published online: 28 October 2023  
© The Author(s), under exclusive licence to Springer Nature Switzerland AG 2023

## Abstract

The primary objective of this study is to develop a geocell-reinforced pavement composition suitable for high-altitude roads using locally available materials and establish a correlation between laboratory and field evaluations. To achieve this goal, the research encompasses the evaluation of layers reinforced with geocell through both laboratory experimental setups and field test sections. In the laboratory, unbound material layers were assembled in a dynamic testing facility with varying compaction levels—specifically, 80%, 90%, and 95%. Subsequent cyclic plate load tests were conducted on these test setup surfaces. The results are notably indicative that the incorporation of geocell led to a significant reduction in permanent deformation within the base layer, resulting in reductions of 10% to 30% across different compaction conditions. Furthermore, this addition of geocell correlated with a noteworthy reduction in base course thickness, ranging from 14 to 50%, aligning with Modulus Improvement Factor (MIF) values ranging from 1.5 to 4. To authenticate the benefits of geocell reinforcement, field sections were constructed, and field California Bearing Ratio (CBR) testing was carried out. The CBR value of the geocell-reinforced field section notably exceeded that of the control section, registering an increase of more than twofold. This augmentation led to a calculated MIF of 1.4. Importantly, the comparison between laboratory and field assessments emphasized that the effectiveness of geocell reinforcement is notably more pronounced in field applications.

**Keywords** Geocell · Relative compaction · Modulus improvement factor · Traffic benefit ratio · Rut depth reduction · Field california bearing ratio

## Introduction

The Himalayan Mountain range extends over several states in North and North-East India. These high-altitude regions have extreme climatic conditions, complex and unsafe terrain, and topography. Additionally, this area has a lower population density and lacks basic infrastructural facilities compared to the plain landscape. As a result, a good and long-lasting road network is critical in Himalayan areas for overall development and to meet defense needs. The design and construction of roads in the high-altitude Himalayan region pose more difficulties than in plain terrain. One of the major problems is the non-availability of suitable quality road construction materials which forced road construction agencies/departments to transport good quality material from long distances, including plains. The practice of transporting material over such long distances is both expensive and not environmentally safe. One probable solution to this problem would be to use locally available materials in the region, which, in most probable

---

✉ Bharath Gottumukkala  
bharat.crrri@nic.in

Bharatram Mehar  
mbharatram@student.nitw.ac.in

Divakar Minchala  
divakarminchala@gmail.com

Subramanya Prasad Pulikanti  
pulikanti@gmail.com

Kranthi Kumar Kuna  
kranthi@iitkgp.ac.in

<sup>1</sup> Flexible Pavement Division, CSIR-CRRI, New Delhi, India

<sup>2</sup> Department of Civil Engineering, Indian Institute of Technology, Kharagpur, Kharagpur, West Bengal, India

<sup>3</sup> Geotechnical Division, CSIR-CRRI, New Delhi, India

occurrences, may be considered marginal due to their inferior quality. Some examples of such locally available materials in the Himalayan region include (i) rocks and gravel obtained during hill cutting or blasting, (ii) Landslide debris, (iii) river-bed material, (iv) tunneling muck, etc. These locally available materials may lack specified gradation or shape, have lower strength, and be weathered due to the environment. While such materials may not have sufficient quality per conventional specifications' requirements, special design considerations can help obtain satisfactory performance. Engineers must use specialized techniques to solve this problem.

Engineers specializing in ground improvement face numerous challenges, compelling them to seek methods that are more reliable, environmentally friendly, and time efficient. Various techniques, such as chemical stabilization, deep mechanical compaction, biological stabilizers, and geosynthetic reinforcement, have been explored [1–4]. However, it is important to acknowledge certain limitations associated with these methods. Chemical stabilizers, although effective, can sometimes pose environmental risks. Biological stabilizers are time dependent and sensitive to environmental conditions, while deep compaction may disrupt underground utilities and lead to differential settlements. Consequently, the utilization of geosynthetics as reinforcement presents a sustainable and eco-friendly solution, particularly for pavement layers, offering an alternative in challenging terrain.

Several authors identified that employing geocell increases load carrying capacity by nearly 65% compared to an unreinforced bed and that the joint strength of the geocell also plays a role in increasing load carrying capacity. Many studies have specified that geosynthetic reinforcement (geotextile, geogrid, and geocell) in the pavement layer can significantly improve pavement performance and reduce base layer thickness [5–14]. Pavement performance can be affected by the type of geosynthetic material and its location, base layer thickness, and subgrade strength [14–16].

The cyclic plate tests conducted on geocell reinforced layers revealed that reinforcement produced better quality and longer-lasting unpaved pavement over poor/soft subgrade materials [17]. A dynamic plate load apparatus was used to simulate traffic loading in a laboratory, and the response to loading was evaluated based on permanent deformation with the number of cycles [18]. In the laboratory tests conducted using a large-size cell, the resilient modulus of coarse and fine-grained soils was evaluated both with and without the presence of geocell reinforcement. The results showed that the type of infill material significantly influenced the impact of reinforcement on the resilient modulus. In the case of sand and gravel, which accumulate long-term strain, the increase in resilient modulus was relatively modest, ranging from 1.4 to 3.2% with coarse-grained infill material. Conversely, with fine-grained infill material (where the soil was confined within the geocell), the resilient modulus experienced

a more substantial increase, ranging from 16.5 to 17.9% during the test [19]. Saride et al. (2013) advocated that geocell reduces plastic deformation (permanent deformation) and improves the Traffic Benefit Ratio (TBR) on the asphalt surface by giving lateral constraint or restraint to the soil [20].

The field studies of geocell reinforced pavement revealed that the rutting was reduced by 36% in comparison with unreinforced section and improved the layer stiffness by 20% [21]. Further the average compressive stresses on the subgrade were significantly reduced in geocell reinforced pavement field sections than with unreinforced sections [22]. Despite the successful implementation of numerous field trials, there is still a limited understanding of the behavior of the combined system, specifically when it comes to quantifying the structural contribution of geosynthetic materials and integrating them into a design methodology. The IRC: SP 59: 2018 guidelines [23] emphasize the importance of the Modulus Improvement Factor (MIF) as a design parameter for geosynthetic pavements. However, not much literature is available that correlates such design parameter between laboratory and field evaluation, particularly for the locally available materials found in the high-altitude regions of India, characterized by hilly terrains. Hence, the objective of the present study is to develop a durable pavement composition that incorporates geosynthetics for high-altitude roads constructed with locally available materials and determine the correlation between laboratory and field evaluation. This shall be achieved through the determination of Modulus Improvement Factor (MIF) and Traffic Benefit Ratio (TBR) both in laboratory and field studies.

In this study, the impact of compaction effort on the performance of geocell-reinforced pavement layers using locally available materials is investigated to understand how different levels of compaction affect the performance of geocell reinforcement. The Modulus Improvement Factor (MIF) is evaluated through the Traffic Benefit Ratio (TBR), using laboratory test data to estimate the reduction in base layer thickness resulting from geocell reinforcement. These results, along with pavement design analysis, were used to guide the installation of field sections in a high-altitude region.

## Materials and methods

### Materials

#### Geocell

For this study, an HDPE geocell was utilized as the reinforcement material. The geocell properties provided by the manufacturer are summarized in Table 1. This information offers a comprehensive overview of the characteristics and specifications of the geocell used in the research.

**Table 1** Geocell properties

Characteristics	Data
Material	High-density polyethylene (HDPE)
Cell depth	150 mm
Sheet wall thickness	1.65 mm
Seam peel strength	2130 N per 150 mm joint
Expanded cell size	259 mm × 224 mm
Expanded section size	2.59 m (W) × 6.50 m (L)
Expanded section area	16.8 m <sup>2</sup>

**Table 2** Properties of soil used in the study

Properties	Value	Test Method
Liquid limit ( $W_L$ )	37%	ASTM D4318-00
Plastic limit ( $W_p$ )	20%	ASTM D4318-00
Plasticity index ( $I_p$ )	17%	ASTM D4318-00
Specific gravity	2.66	ASTM D854-14
Maximum dry unit weight (MDUD)	17.1 kN/m <sup>3</sup>	ASTM D1557-12
Optimum moisture content (OMC)	16%	ASTM D1557-12
CBR value	19%	ASTM D1883-07
Soil classification	CI	IS 1498

### Local soil

The soil used in this study was collected from Manali Sarchu, located near Rohtang Pass in Himachal Pradesh. The geotechnical properties were determined using the standard testing procedures outlined by ASTM in the laboratory. The obtained results can be found in Table 2, providing valuable insights into the soil characteristics utilized in the research.

### Methodology

The study methodology consists of two main phases: Laboratory evaluation and Field evaluation. Initially, soil samples were collected from the high-altitude region and their geotechnical properties were determined.

In the Laboratory evaluation phase, test sections are constructed including both unreinforced and geocell-reinforced pavements, which are compacted at three different levels, corresponding to 80%, 90%, and 95% of Maximum Dry Unit Weight (MDUD), within a large circular tank. The cyclic plate load testing was performed using a servo hydraulic static and dynamic testing machine on the surface of pavement test sections prepared. The results obtained from the laboratory evaluation were analyzed for various factors such as permanent deformation, traffic benefit ratio, reduction in rut depth, modulus improvement factor, and reduction in base layer thickness. These findings were essential

for designing the geocell-reinforced pavements for the field evaluation.

In the phase of field evaluation, both unreinforced and geocell-reinforced pavements were constructed in the Spiti district of Himachal Pradesh, India, which is a high-altitude region. These field sections constructed were subjected to Filed California Bearing Ratio (CBR) testing for the assessment of performance of the pavements (in terms of MIF) in relation to laboratory evaluation. Finally, it was attempted to observe the correlation between the field and laboratory assessment through MIF and thickness reduction in pavement layers. Figure 1 provides an overview of the entire research structure, illustrating how the laboratory evaluation led to the construction and evaluation of geocell-reinforced pavements in the high-altitude region of Spiti, Himachal Pradesh, India.

### Test apparatus and procedure

For this study, a Servo-hydraulic dynamic testing facility, as shown in Fig. 2, was utilized to perform cyclic plate load tests on both reinforced and unreinforced pavement sections. The testing was carried out within a circular tank measuring 1 m in diameter and 1 m in height, equipped with a hydraulic actuator boasting a capacity of 75 kN, and a 70 mm Linear Variable Differential Transformer (LVDT) was employed to measure surface deformations.

In accordance with IRC 37: 2018 guidelines, a seating contact pressure of 0.56 MPa is specifically targeted for application on the pavement surface. To simulate real-time traffic conditions, a trapezoidal loading pattern is employed. This loading pattern, with a frequency of 0.77 Hz [24–26] and a peak magnitude of 10 kN, is applied to a circular steel plate with a diameter of 150 mm. The primary objective of this loading arrangement is to ensure that the resulting tyre pressure aligns precisely with the intended value of 0.56 MPa. Figure 3 clearly illustrates the application of this trapezoidal loading pattern, facilitating a better understanding of the simulation approach used to replicate the real-time traffic and Table 3 describes the test details of the laboratory experiment.

### Edge effect

The impact of edge effects can be disregarded when the width of the loading plate is equal to or less than 1/6th of the width of the tank [27]. In this study, the loading plate utilized had a diameter of 150 mm, which is smaller than 1/6th of the tank width. Therefore, it can be assumed that the edge effects are not significant and can be neglected for the purposes of the analysis.

Fig. 1 Flow Chart of Study

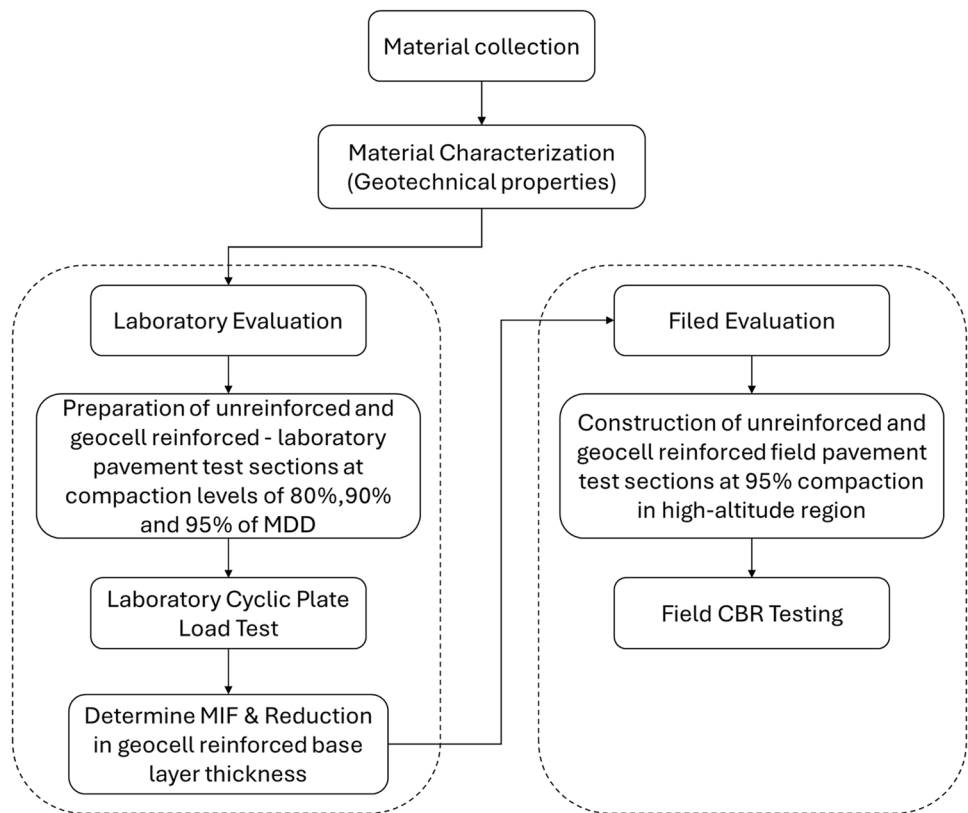


Fig. 2 Plate load testing machine; a Test setup, b Test Tank, c Loading plate

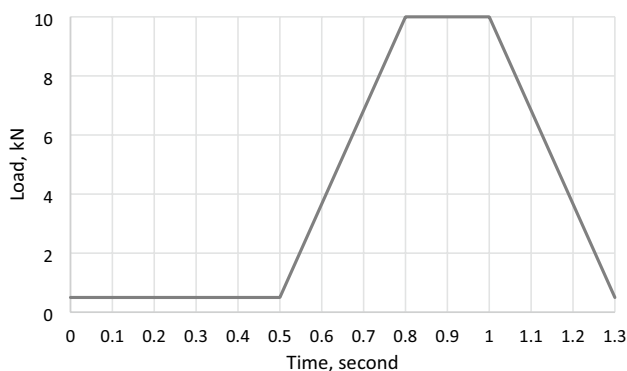


Fig. 3 Loading pattern

**Laboratory sample preparation**

In the large test tank, six sections of unpaved roads were prepared (three without reinforcement and three with geocell reinforcement). Figure 4a depicts the thickness of the subgrade and sub-base material used to construct an unreinforced section in the test tank. The fill material was compacted at three different levels (80%, 90%, and 95% relative compaction as shown in Table 3 to investigate the effect of relative compaction on the laboratory results of the designed pavement section. The subgrade soil was filled in five layers, each of which was 100 mm thick. The soil was compacted to Maximum Dry Unit Weight (MDUD) at corresponding

**Table 3** Laboratory test details

Parameter	Test details
Loading	10 kN (peak)
Seating contact pressure	0.56 MPa
Frequency	0.77 Hz
Loading cycles	18,000
Test section Type	a. Unreinforced pavement section b. Geocell reinforced pavement section
Compaction level	80% of MDUD 90% of MDUD 95% of MDUD

Optimum Moisture Content (OMC). The geocell specimen was then placed on top of the subgrade, followed by two additional layers of fill. The compaction of layers is ensured by achieving the required layer thickness (measured at various locations in the tank) computed from desired unit weight (MDUD) and amount of fill material. Figures 4a and b show the unreinforced and reinforced sections used in this study.

### Results and discussion

Permanent deformation, also known as rutting, serves as a crucial indicator of the performance of the granular base layer within the pavement structure. Consequently, this study places a strong emphasis on evaluating the accumulated permanent deformation resulting from repeated loading. To achieve this, a cyclic plate load test was conducted on both unreinforced and geocell reinforced pavements, constructed within the laboratory, subjected to a maximum of 18,000 loading cycles. Surface deformations were measured using LVDTs (Linear Variable Differential Transformers) and subsequently analyzed in terms of Rut Depth Reduction (RDR)

and Traffic Benefit Ratio (TBR) to determine the effect of reinforcement.

RDR is the ratio of the difference between accumulated permanent deformation of the unreinforced layer ( $D_u$ ) and accumulated permanent deformation of the reinforced layer ( $D_r$ ) to accumulated permanent deformation of an unreinforced layer at a particular repeated load cycle [20]. It is mathematically represented as Eq. (1)

$$RDR = \frac{D_u - D_r}{D_u} * 100 \tag{1}$$

TBR is the ratio of the number of repeated loading cycles to reach a specific rutting in a geocell reinforced layer ( $N_r$ ) to the number of repeated load cycles to reach the same rutting in an unreinforced layer ( $N_u$ ). It is mathematically represented as Eq. (2) [28].

$$TBR = \frac{N_r}{N_u} \tag{2}$$

### Laboratory results

The permanent deformations of both unreinforced and geocell-reinforced sections are computed and depicted in Figs. 5a and b, considering the number of cycles and varying relative compaction. The findings revealed a consistent trend in which the permanent deformation increased with the number of cycles for both the unreinforced and geocell-reinforced layer sections. However, it was notable that the geocell-reinforced layer exhibited less deformation compared to the unreinforced layer. These results align with the conclusions drawn by several researchers [26, 28], further confirming the efficacy of geocell reinforcement in mitigating permanent deformation.

Furthermore, it was observed that both unreinforced and reinforced sections exhibited lower deformation rates in higher relative compacted layers (90% and 95% MDUD) compared to

**Fig. 4** Sample test section, **a** Unreinforced Section **b** Reinforced Section

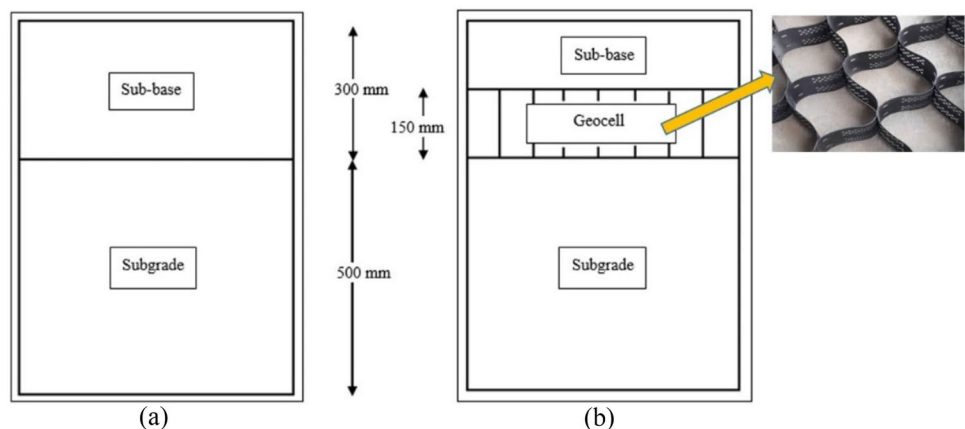




**Fig. 5** Permanent deformation curves of the unreinforced and reinforced sections under varying relative compaction

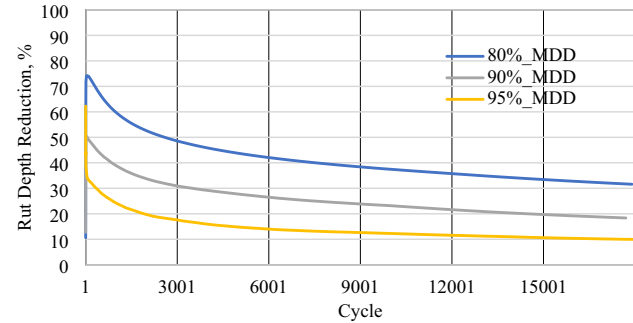
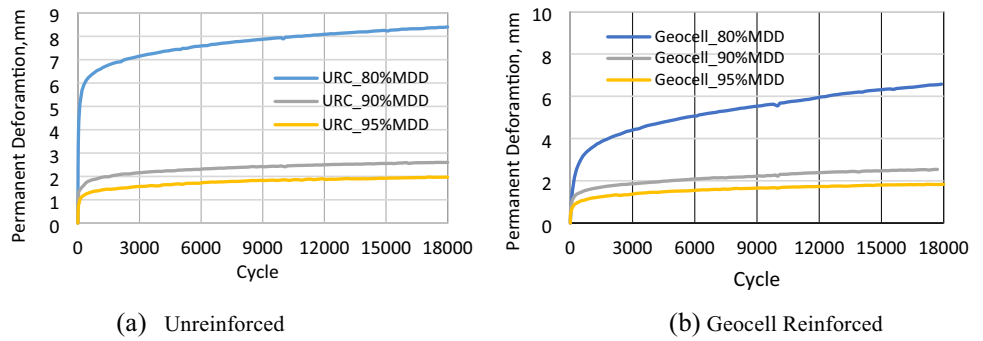


**Fig. 6** Variation of RDR v/s Cycle for different relative compaction

loosely compacted layers (80% MDUD) due to the presence of higher voids in the latter. Moreover, the reduction in permanent deformation i.e., RDR, reaches to a constant value of 31% at 80% relative compaction, 18% at 90% relative compaction and 10% at 95% relative compaction compared to the unreinforced section (Fig. 6) at 18000th load cycle. These results indicate that densely compacted layers (90% and 95% MDUD) experience lower deformations, while the impact of reinforcement is more pronounced in loosely compacted layers (80% MDUD). This can be attributed to the geocell reinforcement's ability to provide enhanced lateral confinement, particularly benefiting the loosely compacted layers by effectively engaging with the aggregates.

The evaluation of pavement reinforcement benefits is essential in understanding its impact on the extended life of pavements and the reduction in base layer thickness [5–7, 29]. To quantify these advantages, the Traffic Benefit Ratio (TBR) is computed, utilizing experimental data, and considering various permanent deformation criteria at different levels of relative compaction. Equation (2) is applied to estimate the TBR values, while Tables 4, 5, 6 provide specific TBR values corresponding to 80%, 90%, and 95% relative compaction, respectively. The increase in permanent deformation leads to an increase in TBR values for 80% and 90% relative compaction, whereas for 95% relative compaction, TBR values decrease with an increase in permanent deformation. This phenomenon can be attributed to the fact that in

**Table 4** TBR value at 80% relative compaction

Permanent deformation, mm	Cycle		TBR
	URC	Geocell	
1	5	42	8
2	6	161	20
3	14	491	35
4	32	1831	57
5	87	5553	64

**Table 5** TBR value at 90% relative compaction

Permanent deformation, mm	Cycle		TBR
	URC	Geocell	
1	16	174	11
1.5	99	1633	16

**Table 6** TBR value at 95% relative compaction

Permanent deformation, mm	Cycle		TBR
	URC	Geocell	
1	93	408	4
1.5	2209	5228	2

the case of a highly dense layer (95% relative compaction), the increasing load cycles result in further densification, which mitigates the impact of reinforcement.

Moreover, the study revealed noteworthy findings with regards to TBR values, indicating that they were markedly higher for lower compaction levels [30]. This suggests that the advantages of incorporating geocell reinforcement are particularly pronounced when dealing with lower compaction levels or soils that are more compressible. However, it is important to note that lower compaction levels can result in reduced field CBR values, increased potential for water percolation due to higher voids, erosion, and consequently, heightened permanent deformation. Furthermore, the computed TBR values are utilized to determine the modulus

improvement factors for the design of geocell reinforced pavements.

### Modulus improvement factor (MIF)

Modulus Improvement Factor (MIF) is one of the key design parameters in the design of geosynthetic reinforced pavement design. It is the increase in modulus of the layer due to incorporation of geosynthetics. MIF can be defined as the ratio of modulus of geosynthetic reinforced layer ( $E'_{GSB}$ ) to the modulus of unreinforced layers ( $E_{GSB}$ ). The moduli of both geocell reinforced and unreinforced layers were determined using layer coefficient equation recommended by the American Association of State Highway and Transportation Officials (AASHTO) in their pavement design guidelines [31]. As per AASHTO (1993), the pavement is treated as a multilayer elastic system with an overall Structural Number (SN), taking resilience and overall pavement stability under repeated loads into account. The overall Structural Number (SN) derived from this approach is then used to determine the layer coefficient for both geocell reinforced and unreinforced layers. The computation procedure for the Modulus Improvement Factor (MIF) is as follows.

In accordance with AASHTO (1993) guidelines, traffic is characterized in terms of 18-kip Equivalent Standard Axle Loads (ESALs) and represented as  $W_{18}$ . For this study, three different traffic levels (18-kip ESALs) of 2,000,000; 5,000,000; and 10,000,000 were considered for the unreinforced pavement layers, denoted as  $W_{18,unreinforced}$ . The traffic or design life for reinforced pavements ( $W_{18,reinforced}$ ) was computed by varying the TBR values from 1 to 10 using Eq. (3).

$$W_{18,reinforced} = TBR * W_{18,unreinforced} \tag{3}$$

The structural number of the pavement layer is determined using Eq. (4) as outlined in the AASHTO (1993) guidelines.

$$\begin{aligned} \text{Log}W_{18} = & Z_R S_O + 9.36 \log(\text{SN} + 1) \\ & - 0.2 + \log \left\{ \log \left( \frac{\Delta PSI}{2.7} \right) / \left( 0.4 + \frac{1094}{\text{SN} + 1} \right) 5.9 \right\} \\ & + 2.32 \log M_R - 0.87 \end{aligned} \tag{4}$$

where  $W_{18}$  is the Estimated cumulative 18-kip ESAL during the design life of the pavement,  $S_O$  is the overall standard deviation,  $Z_R$  is the standard normal deviate for reliability level,  $\Delta PSI$  is the allowable loss in serviceability, and  $M_R$  is the resilient modulus of the underlying subgrade. Considered the standard deviation = 0.45, reliability = 95%,  $\Delta PSI = 1.7$ , and subgrade modulus = 116 MPa are used for this study for both unreinforced and reinforced layer.

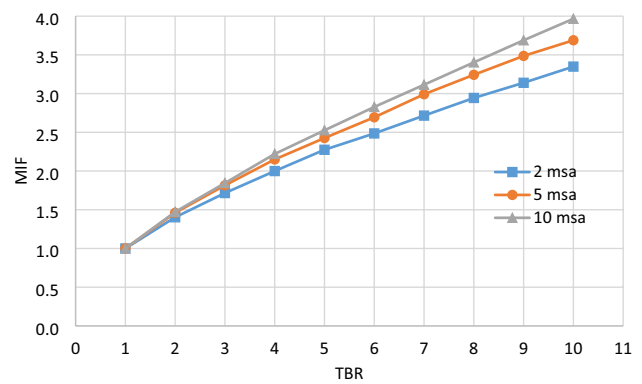


Fig. 7 Variation for MIF versus TBR for different design traffic

After computing the structural number (SN), the layer coefficients for unreinforced ( $a_3$ ) & reinforced ( $a_3'$ ) sections [31] are determined using Eqs. (5) and (6), respectively.

$$SN = a_1 d_1 + a_2 d_2 m_2 + a_3 m_3 d_3 \tag{5}$$

$$SN = a_1 d_1 + a_2 d_2 m_2 + a_3' m_3 d_3 \tag{6}$$

where, SN = Overall Structural Number which is the total calculated strength of the pavement layers,  $a$  = Layer coefficient,  $d$  = Layer thickness (in inches).

Calculate the modulus of the unreinforced sub-base layer ( $E_{GSB}$ ) using Eq. (7) and modulus of the reinforced sub-base layer using Eq. (8) [31].

$$a_3 = 0.277 (\log_{10} E_{GSB}) - 0.839 \tag{7}$$

$$a_3' = 0.277 (\log_{10} E'_{GSB}) - 0.839 \tag{8}$$

Once the modulus values have been obtained for both the reinforced and unreinforced sections, the Modulus Improvement Factor (MIF) is calculated using Eq. (9) [32]. This factor allows for the comparison of the modulus enhancement resulting from the incorporation of reinforcement.

$$MIF = \frac{E_{GSB}}{E'_{GSB}} \tag{9}$$

A chart depicting the Modulus Improvement Factor (MIF) was developed in this study (Fig. 7) under different design traffic levels in million standard axles (msa), i.e., 2, 5, and 10 msa with varying TBR values ranging from 1 to 10. The findings revealed that as the TBR increased, along with the design traffic, the MIF value also increased which indicates that the strength of the pavement layers improved due to the incorporation of geocell reinforcement. The MIF chart serves as a visual representation of the enhanced modulus resulting from the use of geocell reinforcement and provides valuable insights for the pavement design process.

## Base course thickness reduction

The utilization of geocell reinforcement in flexible pavements aims to achieve a dual objective: reducing the required amount of base course material while simultaneously enhancing performance and prolonging the pavement's lifespan. In the current study, a pavement design with a traffic of 10 msa, the reduction in base course thickness was determined for varying MIF values, ranging from 1 to 4. The modulus of the unreinforced section was computed using Eq. (10) proposed by the IRC 37 (2018) guideline for the base or subbase layer [32]. Additionally, Eq. (11) is utilized to calculate the modulus of the reinforced section, taking MIF into account.

$$E_{unreinforced} = 0.2 * h^{0.45} * E_{SG} \quad (10)$$

$$E_{reinforced} = MIF * E_{unreinforced} \quad (11)$$

where,  $E_{SG}$  = Elastic modulus of subgrade,  $h$  = thickness of base and sub-base layer.

In this study, the bituminous and subbase course thicknesses were kept constant, and the pavement analysis is carried out as per IRC 37: 2018. Initially, the design and analysis were carried out for the unreinforced section and the obtained value of vertical strain for the unreinforced layer was used for determining the thickness of reinforced layer required for obtaining the same vertical strain by varying the MIF values. The reduction in base course thickness (as depicted in Fig. 8) ranged from 14 to 50%, corresponding to MIF values of 1.5 to 4, respectively. This approach allowed for a comprehensive assessment of the impact of different MIF values on the required thickness of the base course, providing valuable insights for optimizing pavement design and resource utilization.

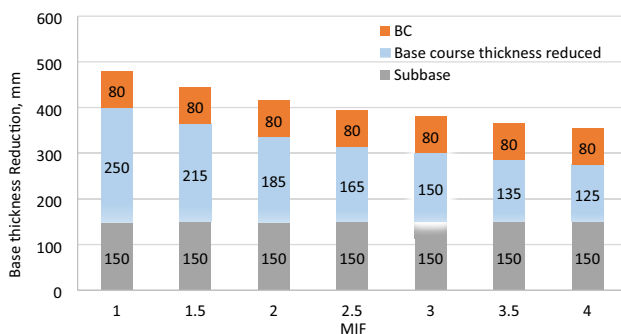


Fig. 8 Reduction of base thickness with Geocell

## Field evaluation of unreinforced and geocell reinforced pavements

A field study was conducted in the Spiti District of Himachal Pradesh, India, to assess the performance of geocell reinforcement in comparison to unreinforced sections. Two test sections with a design life of 10 msa, each measuring 100 m in length, were constructed for this purpose and the geocell of the same material and dimension used in the laboratory was employed in the field section too. The subgrade, sub-base, and base layers in both sections were compacted to 95% of the Maximum Dry Unit Weight (MDUD) at their respective optimum moisture contents (OMC) using pneumatic tyred rollers. Figure 9 provides a visual representation of a typical geocell reinforced (GR) and unreinforced (UR) pavement section, highlighting the subgrade and granular layers. In the geocell reinforced section, the base layer had a thickness of 100 mm, resulting in a 33% reduction in base layer thickness and an overall reduction of the granular layer thickness compared to the unreinforced section. This reduction in thickness is to evaluate the potential benefits of geocell reinforcement in optimizing material usage.

The construction of the geocell-reinforced pavement section began with the preparation of a smooth roadbed, followed by the placement of the geocell. Subsequently, fill material was deposited into the geocell pockets using loading trucks. After filling, the surface was scraped to ensure a smooth finish, and then compacted to reach 95% MDUD using a pneumatic tyred roller. For a more explicit depiction of the field construction process of the geocell-reinforced pavement, please refer to Fig. 10a. These field observations and measurements contribute to a comprehensive understanding of the performance and practical application of geocell reinforcement.

Field California Bearing Ratio (CBR) tests were conducted on the granular layer of pavement to evaluate the benefits of geocell reinforcement (Fig. 10b). A field CBR test was performed on the granular layer's surface to determine the bearing strength of the base course in accordance with ASTM D4429-04 which is given by Eq. (12).

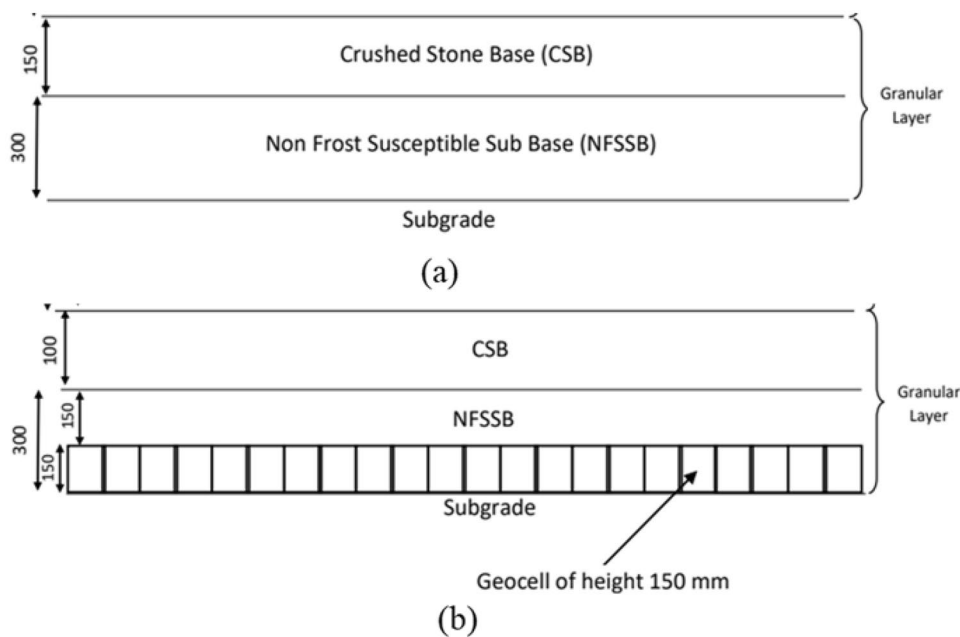
$$CBR = \frac{P_t}{P_s} * 100 \quad (12)$$

where  $P_t$  = test load of corresponding penetration, and  $P_s$  = standard load of crushed aggregate for the same penetration.

Figure 11 illustrates the load-deformation curves obtained for both the geocell reinforced and controlled unreinforced sections. A notable observation is the significant increase in load with penetration for the GR section compared to the UR section. This improvement can be attributed to the three-dimensional confinement effects of the geocell walls, which



**Fig. 9** Typical pavement sections constructed in the field. **a** control section (UR); **b** GR section



(a)



(b)

**Fig. 10** Field evaluation **a** Laying of Geocell reinforcement in field, **b** Field CBR test

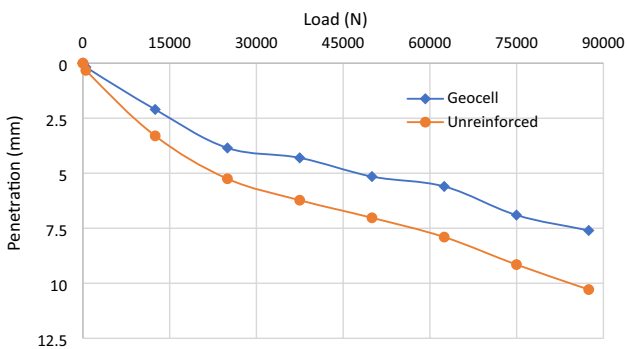


**Fig. 11** Load versus deformation plot

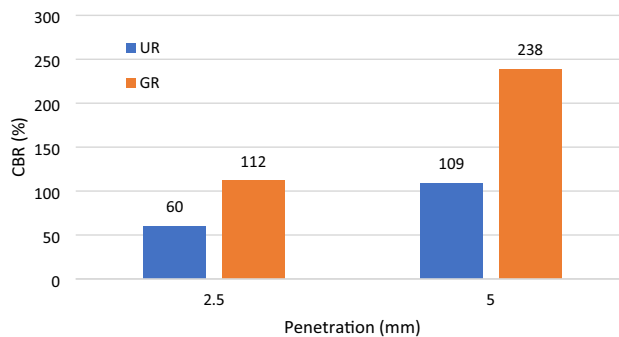


**Fig. 12** CBR versus penetration plot

result in a wider distribution of stress. A similar behavior was reported by Han et al. (2011) in their study on geocell reinforced RAP bases over weak subgrade [33].

To further evaluate the performance, CBR values were calculated using Eq. (12) based on the standard load at penetration depths of 2.5 mm and 5 mm, along with their corresponding loads. Figure 12 presents the plot of CBR values against penetration for both sections and it is evident that the CBR values of the base layers in the GR sections were more than doubled compared to the control section, at both the 2.5 mm and 5 mm penetration depths. The improvement in CBR of GR section was computed and it was found that CBR of GR section is 2.18 times (i.e., percentage increase in CBR = 118.35%) CBR of UR section. This enhancement in field CBR signifies the ability of geocell reinforcement to accommodate higher traffic loads and increase the pavement's design life when compared to an unreinforced case [34].

The increase in the CBR of the GR section serves as a basis for calculating the enhancement in the GR section's modulus. This improvement is quantified by the modulus improvement factor and computed using the Eq. (13) [35].

$$E_B = 29.4 * CBR^{0.4358} \quad (13)$$

With a CBR increase of 118.35% in the GR section, the resulting modulus increment in the GR section is determined to be 1.41 times the modulus of the UR section, i.e., MIF = 1.41, utilizing Eq. (13). An attempt is made to establish a correlation between the field evaluation and laboratory assessment, which is accomplished by identifying the TBR value through laboratory evaluations and aligning it with the MIF value determined during the field evaluation.

From Fig. 7, the chart depicting the Modulus Improvement Factor (corresponding to 10 MSA), the TBR corresponding to MIF = 1.41 is approximately 1.9. This can be interpreted to mean that a TBR of 1.9 in the laboratory assessment may result in a modulus increment of 1.41 times for the GR field section (i.e., MIF = 1.41) in comparison with the UR section.

Laboratory evaluation (from Fig. 8) reveals that with a geocell having MIF = 1.5, the granular layer thickness of the pavement can be reduced by 8.8%. However, an overall thickness reduction of 11% in the granular layer of the field GR section resulted in MIF = 1.41. This indicates that the incorporation of geocell in the pavement layers outperformed in the field application compared to the laboratory application. These findings reinforce the effectiveness of geocell reinforcement in enhancing the structural response and longevity of pavements, validating its potential for practical application in various pavement engineering projects.

## Conclusions

In this study, laboratory tests were conducted on locally available soil materials in high-altitude regions to investigate the effects of incorporating geocells into the base layer of pavements on performance enhancements, including TBR, RDR, and MIF. Cyclic plate load tests were conducted on both reinforced and unreinforced sections at compaction levels of 80%, 90%, and 95%. The study's conclusions are outlined below:

- The reinforced sections demonstrated notably reduced permanent deformation, particularly at lower compaction levels. The influence of reinforcement was most pronounced at lower compaction levels compared to higher compaction (95% MDUD). The RDR decreased and stabilized at values of 31% for 80% relative compaction, 18% for 90% relative compaction, and 10%

for 95% relative compaction. Furthermore, base course thickness reductions ranged from 14 to 50% for MIF values of 1.5 to 4.

- Field sections, both geocell-reinforced (GR) and unreinforced (UR), were constructed in the high-altitude region at 95% compaction, with field CBR measurements taken for performance validation. The CBR of the geocell-reinforced layers exceeded that of the control (UR) pavement section by a factor of two. The geocell-reinforced pavement outperformed the unreinforced section, resulting in a 33% reduction in base layer thickness and an 11% reduction in overall granular layer thickness.
- Furthermore, geocell's performance was found to be more effective in field applications than in laboratory simulations.
- In summary, this study successfully demonstrates the effective utilization of locally available soil materials in high-altitude regions, incorporating geocell reinforcement in the base layer to enhance pavement performance under increased design traffic conditions. Additionally, this approach offers advantages in terms of cost savings in transportation, time efficiency, and a reduced carbon footprint.

## Limitation

The main limitation of the study is that the laboratory and field evaluations are not validated for the repeatability due to the laborious work of constructing the pavement test section both in the laboratory and field.

**Acknowledgements** The authors are thankful to Director, CSIR – CRRI, New Delhi, for his kind permission to publish this paper. We thankfully acknowledge GBPNHIESD, which gave us financial assistance for the project work.

**Author contributions** GB conceived the study and was responsible for the design and development of the data analysis. GB and MB were responsible for testing, data collection and analysis. MD, PSP and KKK were responsible for data interpretation. MB and PSP were responsible for the preparation of the draft, while MD, GB and KKK were responsible for preparation of final manuscript.

**Funding** This work was supported by the G.B. Pant National Institute of Himalayan Environment and Sustainable Development (GBPNHIESD) under Grant GBPNHIESD-2017–18/MG-30.

**Data availability** The datasets generated during and/or analyzed during the current study are available from the corresponding author on reasonable request.

## Declarations

**Conflict of interest** There are no conflicts of interest between the authors with other entities or researchers.

## References

- Verma H, Ray A, Rai R, Gupta T, Mehta N (2021) Ground improvement using chemical methods: a review. *Heliyon* 7(7):e07678
- Alimohammadi H, Amirmojahedi M, Tahat JN (2022) A case history of application of deep compaction method with comparison to different ground improvement techniques. *Transp Infrast Geotechnol* 5:52
- Dhanya JS, Fouzul MA, Banerjee S, Boominathan A, Zhusupbekov A (2023) Shaking table experiments on framed structure resting on geogrid reinforced geotechnical seismic isolation system. *Bull Earthquake Eng*. <https://doi.org/10.1007/s10518-023-01687-x>
- Aliasgharzadeh M, Yousefzadehfard M, Atrchian M, Bayat M (2023) Experimental study on pullout capacity of geocell and geotextile-reinforced horizontal plate anchors embedded in granular soil. *Int J Geosynth Ground Eng* 9(1):6
- Tingle JS, Jersey SR (2005) Cyclic plate load testing of geosynthetic reinforced unbound aggregate roads. *Transp Res Rec* 1936(1):60–69
- Chen Q, Abu-Farsakh M, Tao M (2009) Laboratory evaluation of geogrid base reinforcement and corresponding instrumentation program. *Geotech Test J* 32(6):516–525
- Perkins SW, Christopher BR, Cuelho EL, Eiksund GR, Schwartz CS, Svanø G (2009) A mechanistic–empirical model for base reinforced flexible pavements. *Int J Pavement Eng* 10(2):101–114
- Jersey SR, Tingle JS, Norwood GJ, Kwon J, Wayne M (2012) Full scale evaluation of geogrid reinforced thin flexible pavements. *Transp Res Rec* 2310(1):61–71
- Tang X, Abu-Farsakh M, Hanandeh S, Chen Q (2015) Performance of reinforced–stabilized unpaved test sections built over native soft soil under full scale moving wheel loads. *Transp Res Rec* 2511(1):81–89
- Tang X, Stoffels SM, Palomino AM (2013) Resilient and permanent deformation characteristics of unbound pavement layers modified by geogrids. *Transp Res Rec* 2369(1):3–10
- Tanyu BF, Aydilek AH, Lau AW, Edil TB, Benson CH (2013) Laboratory evaluation of geocell reinforced gravel subbase over poor subgrades. *Geosynth Int* 20(2):47–61
- Abu-Farsakh M, Hanandeh S, Mohammad L, Chen Q (2016) Performance of geosynthetic reinforced/stabilized paved roads built over soft soil under cyclic plate loads. *Geotext Geomembr* 44(6):845–853
- Saghebfar M, Hossain M, Lacina BA (2016) Performance of geotextile reinforced bases for paved roads. *Transp Res Rec* 2580(1):27–33
- Kumar VV, Saride S (2016) Rutting behavior of geocell reinforced base layer overlying weak sand subgrades. *Proced Eng* 143:1409–1416
- Perkins SW (1999). Geosynthetic reinforcement of flexible pavements: laboratory based pavement test sections (No. FHWA/MT-99-001/8138). Montana. Department of Transportation.
- Al-Qadi IL, Dessouky SH, Kwon J, Tutumluer E (2008) Geogrid in flexible pavements: validated mechanism. *Transp Res Rec* 2045(1):102–109
- Pokharel SK (2010). Experimental study on geocell reinforced bases under static and dynamic loading (Doctoral dissertation, University of Kansas).
- Benjamim C, Bueno B, Zornberg JG (2007) Field monitoring evaluation of geotextile reinforced soil retaining walls. *Geosynth Int* 14(2):100–118
- Mengelt MJ, Edil TB, Benson CH (2006) Resilient modulus and plastic deformation of soil confined in a geocell. *Geotext Geomembr* 13(5):195–205
- Saride S, Rayabharapu V, Vedpathak S Puppala AJ (2013). Repeated load tests on geocell reinforced sand subgrades. *Geosynthetics*, April 1st–4th. Long Beach, California, pp. 400 – 409.
- Khan MA, Puppala AJ (2023) Sustainable pavement with geocell reinforced reclaimed-asphalt-pavement (RAP) base layer. *J Clean Prod* 387:135802
- Khan MA, Biswas N, Banerjee A, Puppala AJ (2020) Field performance of geocell reinforced recycled asphalt pavement base layer. *Transp Res Rec* 2674(3):69–80
- IRC SP. 59. (2019). Guidelines for use of geosynthetics in road pavements and associated works. In the Indian Road Congress, New Delhi.
- Abu-Farsakh M, Souci G, Voyiadjis GZ, Chen Q (2012) Evaluation of factors affecting the performance of geogrid-reinforced granular base material using repeated load triaxial tests. *J Mater Civ Eng* 24(1):72–83
- Qian Y, Han J, Pokharel SK, Parsons RL (2013) Performance of triangular aperture geogrid reinforced base courses over weak subgrade under cyclic loading. *J Mater Civ Eng* 25(8):1013–1021
- Thakur JK, Han J, Parsons RL (2017) Factors influencing deformations of geocell reinforced recycled asphalt pavement bases under cyclic loading. *J Mater Civ Eng* 29(3):04016240
- Hegde A, Sitharam TG (2015) Effect of infill materials on the performance of geocell reinforced soft clay beds. *Geomech Geoen Int J* 10(3):163–173
- George AM, Banerjee A, Puppala AJ, Saladhi M (2021) Performance evaluation of geocell reinforced reclaimed asphalt pavement (RAP) bases in flexible pavements. *Int J Pavement Eng* 22(2):181–191
- Berg, R.R. (2000). Geosynthetic Reinforcement of the Aggregate Base/Subbase Courses of Pavement Structures. Geosynthetic Materials Association, Roseville, MN, USA, 176p.
- Pokharel SK, Han J, Leshchinsky D, Parsons RL (2018) Experimental evaluation of geocell reinforced bases under repeated loading. *Int J Pavement Res Technol* 11(2):114–127
- AASHTO (1993) Guide for design of pavement structures. American Association of State Highway and Transportation Officials, Washington, DC
- IRC: 37. (2018). Guidelines for the design of flexible pavements (Fourth Revision). In Indian Roads Congress, New Delhi, India.
- Han J, Pokharel SK, Yang X, Manandhar C, Leshchinsky D, Halahmi I, Parsons RL (2011) Performance of geocell-reinforced RAP Bases over weak subgrade under full-scale moving wheel loads. *J Mater Civ Eng* 23(11):1525–1534
- Pokharel, S.K., Martin, I., Norouzi, M. and Breault, M. (2015). Validation of geocell design for unpaved roads. In Proceedings of Geosynthetics (pp. 15–18).
- Han J. (2015). Principles and practice of ground improvement. Ed. John Wiley & Sons Wiley. <https://doi.org/10.1007/s13398-014-0173-7.2>

**Publisher's Note** Springer Nature remains neutral with regard to jurisdictional claims in published maps and institutional affiliations.

Springer Nature or its licensor (e.g. a society or other partner) holds exclusive rights to this article under a publishing agreement with the author(s) or other rightsholder(s); author self-archiving of the accepted manuscript version of this article is solely governed by the terms of such publishing agreement and applicable law.